Multidisciplinary System Optimization of a Spacecraft Interferometer Testbed

Deborah J. Howell* and Olivier de Weck, Ph.D.†

MIT Dept. of Aeronautics and Astronautics, Cambridge, MA 02139, USA

I. Abstract

This paper applies existing multidisciplinary system design optimization (MSDO) techniques (DOE, gradient based optimization, sensitivity analysis and heuristic techniques) to a spacecraft interferometer testbed in order to minimize the pointing error while keeping a minimum optical pathlength. It is shown that minimizing pointing error does not necessarily drive the optical pathlength. Also insights (such as pointing error sensitivities to particular design variables) are revealed using MSDO techniques. A comparison on the appropriateness of different optimization techniques (gradient search, heuristic search) as applied to this problem is performed.

II. Introduction

Simulation is a key tool that is used to evaluate the tradespace for complex opto-structural systems, such as space telescopes. The Space Interferometry Mission (SIM; currently being developed by NASA with a projected launch date of 2009) relies heavily on simulation.[10] Building test articles for space telescopes are prohibitively expensive and sometimes infeasible in a 1-g environment, therefore simulation becomes very important, and design decisions are based on those simulation results. Optimization can be used in conjunction with simulation in order to map out the effects of changing design variables, and ultimately to help choose a design which best fits requirements or performs the best. There are many different measures of "best", and this definition is part of the optimization process.

An interferometer is a type of telescope that collects light from a star (or other light source) in two or more different locations, combines that light, and measures the optical pathlength difference (measured in wavelengths of light) between light beams in order to collect information (position and distance from Earth) about that star. Spacecraft interferometers will determine the distance to stars several hundred times more accurately than existing monolithic mirror telescopes. For example, the accuracy of SIM is projected to be 4 microarcseconds. The accuracy of the telescope is directly related to the distance between the light collectors; the further apart the light collectors are, the more accurate the telescope. The distance the light travels between collectors is called optical pathlength (OPL). The physical attributes (flexibility, stiffness, etc.) of the structure connecting the the light collectors introduces pointing error (PE) into the light combining system, a key performance metric for spacecraft interferometers.

Figure 1. Artist's Concept of SIM

An investigation into the conceptual design of spacecraft interferometers is presented in this paper. The relationships between PE, OPL, and other design parameters are examined using truss structures comparable to spacecraft structures. The initial objective function will be to minimize the pointing error. The OPL, and therefore the collector positions, is considered variable. Other design variables include controller gain, spacecraft mass and disturbance level. The overall objective of this paper is to effectively evaluate the

*Ph.D. Candidate, MIT Dept. of Aeronautics and Astronautics, 77 Mass. Ave., 37-346, Cambridge MA 02139

†MIT Assistant Professor of Aeronautics and Astronautics and Engineering Systems Division

tradespace for a spacecraft interferometer in the conceptual design phase using existing MSDO techniques. The multi-objective optimization problem will be addressed by adding the maximization of the OPL to the objective function.

III. Project Description

The case study presented here is based on a testbed that structurally represents a spacecraft interferometer (OPTSIM). This complex system incorporates the disciplines of structures, disturbance, optics,

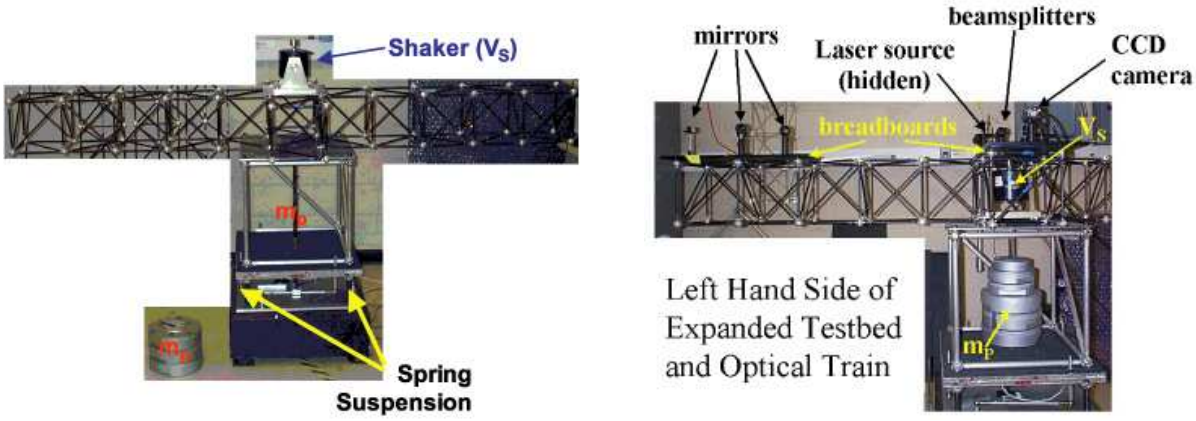

(a) (b)

Figure 2. (a) OPTSIM (b) Optical Train

thermodynamics, and control. The testbed has a central area, where most of the weight is located (spacecraft bus weight, Mp), and a long truss on which the optics reside. It also has a shaker, which represents the disturbance forces occurring on orbit (primarily due to reaction wheels). The disturbance level of the shaker is determined through the input voltage (Vs). The optical train is made up of mirrors, beamsplitters, a CCD camera, and a laser source (He-Ne 635nm 5mW).[3] Gathering interferometric data on actual starlight requires that the light be collected at each end of the long truss. In the lab however this is simulated by splitting laser light and reflecting it to each end of the truss.

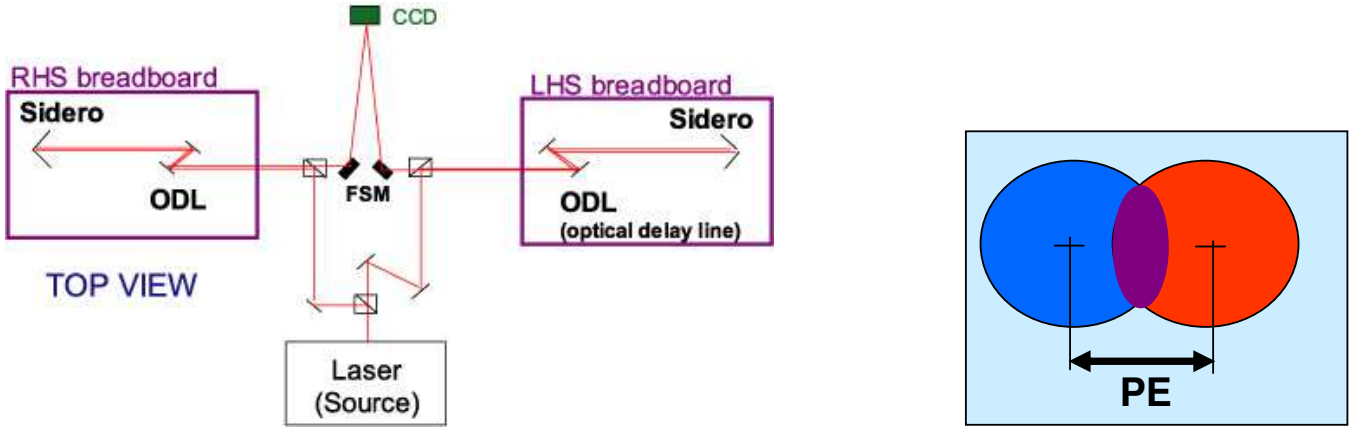

(a) (b)

Figure 3. (a) Optical Layout: Top View (b) CCD plane

The light is then reflected back towards the center and collected on the CCD camera (see Figure 3 (a)). Also depicted are optical delay lines (ODL). They consist of optical elements which move in order to change the length of the light path. The optical delay lines in this paper are assumed to be stationary throughout, however their existence in this model makes it easier to implement control of the optical path length in the future. In order for science data to be collected from an interferometer, two different light paths must first of all overlap on the detector, so that fringes might be detected. The area of overlap is called beam shear (see Figure 3(b)). The distance between the centroids of the beam is called pointing error (PE). Generally, for interferometers, the baseline length is determined by the accuracy requirement. However, in this study, the baseline length (and therefore optical pathlength) is be considered flexible. This is accomplished by assigning the placement of the two outermost (AKA siderostat) mirrors as design variables (M1, M2).

The control scheme is also incorporated into the design vector. The controller will adjust the angular position of the fast-steering mirrors (FSM) which reflect the light from the ends of the truss bays onto the CCD camera. This controller is designed to control the pointing error only. The three control design variables are the values of the control gains for proportional, integral, and derivative control ($\underline{K} = [K1\ K2\ K3]^T$).

The single objective in this study is to minimize the pointing error. The optical pathlength (OPL) and optical pathlength difference (OPLD) are set here as constraints, but can be later added to the objectives. The lower bound on pathlength ensures that the pathlength is long enough so that the testbed still reasonably resembles a spacecraft interferometer (i.e. a long truss segment). In addition, the longer the pathlength, the better the overall telescope accuracy. The pathlength value describes one path of the split beam. The OPLD describes the difference between the lengths of the right hand side and left hand side beams. For interferometry, this value generally needs to be about 1/20th of the wavelength of the light collected. The single objective problem statement is shown in Equation 1.

$$\begin{aligned} &\min PE = \mathrm{PE}(\underline{K},\ \mathrm{M1},\mathrm{M2},\ \mathrm{Mp},\ \mathrm{Vs}) \\ &\text{subject to: } \mathrm{OPLD} < 20 \text{ nm} \ ,\ \mathrm{OPL} > 3\mathrm{m},\ \max(\underline{K}) \leq 100 \end{aligned} \tag{1}$$

The siderostats are placed on optical breadboards, that are bolted to the truss. These mirrors can be moved easily to different discrete locations within certain limits. The values for the location coordinates will be in increments of one inch, since that is the spacing of the breadboards. Conceivably, rails could be used so that the coordinates would be continuous. This option could be used if a chosen optimization routine is too difficult to reasonably implement with incremental values for the coordinates. A detailed finite element

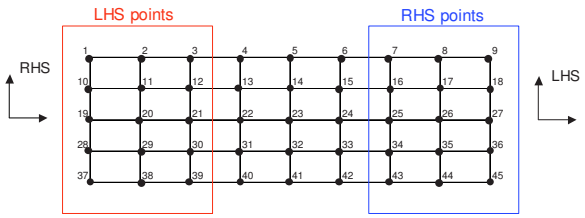

Figure 4. Breadboard layout

model of the testbed will be used in this optimization.

IV. Simulation Model Setup and Integration

For the simulation model, the disciplines of structures, disturbance, optics, and control are represented. All of these modules can be simulated inside the MATLAB® environment using IMOS (Integrated Modeling of Optical Systems). IMOS is a finite element and optical software package that was developed at NASA Jet Propulsion Lab. IMOS is a collection of .m files that allows the designer to construct the multidisciplinary model in one environment.[7] In addition, since it is based in MATLAB®, it will be easy to integrate with optimization routines in MATLAB®. The disturbance block is modelled using empirical data of the shaker on the testbed. The structural module is a finite element model built using material properties and geometric parameters of the components of the testbed. A wireframe model of the testbed is shown in Figure 5. An optical program (*optrace*) was used to determine the placement of each of the beams on the focal plane (in this case the CCD camera). This information is then used to calculate the pointing error.

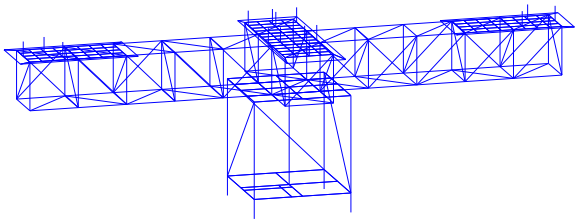

Figure 5. Structural FE Model

Since the structures are conveniently modelled in state space, an optical sensitivity matrix for each structural configuration was constructed using *optrace*. The sensitivity matrix relates the angular displacements of the siderostat mirrors to the pointing error. Several different stepsizes of the angular displacements were tried in order to get an appropriate sensitivity matrix. Using this matrix, the outputs of the structural state space model could be related directly to the pointing error.

$$\dot{\underline{x}} = \mathbf{A}\underline{\mathbf{x}} + \mathbf{B}\underline{\mathbf{u}}$$
$$\underline{y} = \mathbf{C}\underline{\mathbf{x}}$$
$$\underline{z} = \mathbf{FC}\underline{\mathbf{x}}$$

where $\mathbf{A}$ is the system matrix, $\mathbf{B}$ is the input matrix, $\underline{x}$ is the state vector, $\underline{y}$ is the output vector (that contains the angles of the siderostat mirrors), $\mathbf{F}$ is the optical sensitivity matrix (OSM), and $\underline{z}$ is the pointing error. The two fast steering mirror (FSM) angles (θ_1, θ_2) will be controlled in order to steer the beam to the nominal operating point. The output of the controller will be the actual angles that the FSM's steer through (ϕ_1, ϕ_2). This will then alter the OSM, and the pointing error will be controlled.

In the initial DOE exploration, the objectives are calculated in an open-loop system, and only the first four entries of the design vector (the x and y positions of the two siderostat mirrors) are explored. Each of these factors are divided into three levels. For the x positions, the first level will be the nominal level, and the second and third levels will move closer to the origin in steps of 0.0625 m. For the y values, the first level will be the nominal position, and the second and third will be minus and plus 0.0625 m respectively. This is because the optical breadboard is modelled with a meshing fineness of 0.0625 m in the structural module. This does not include all the mirror placement possibilities, but focuses on the outermost region of each breadboard, and will suffice for an initial exploration. An orthogonal array will be used to explore this design space because it is suspected that these factors effect each other. The array and its results can be seen in Tables 1 and 2.

Table 1. Orthogonal Array

1	$x1_1$	$y1_1$	$x2_1$	$y2_1$
2	$x1_1$	$y1_2$	$x2_2$	$y2_2$
3	$x1_1$	$y1_3$	$x2_3$	$y2_3$
4	$x1_2$	$y1_1$	$x2_2$	$y2_3$
5	$x1_2$	$y1_2$	$x2_3$	$y2_1$
6	$x1_2$	$y1_3$	$x2_1$	$y2_2$
7	$x1_3$	$y1_1$	$x2_3$	$y2_2$
8	$x1_3$	$y1_2$	$x2_1$	$y2_3$
9	$x1_3$	$y1_3$	$x2_2$	$y2_1$

These results were evaluated with a bus mass of 200 lbs. and a shaker voltage of 1.0 Vrms. The smallest pointing error obtained was 0.005m, and the largest optical pathlength obtained was about 4.1m. None of the configurations violated the lower bound on the pathlength of 3m. Only one of the configurations met the OPLD constraint of 20nm.

Table 2. Orthogonal Array Results

	PE (m)	OPL (m)	OPLD(μm)
1	0.0244	4.1086	2.1230
2	0.0005	4.0448	-0.72000
3	0.0494	3.9848	0.018000
4	0.0370	3.9842	3.9020
5	0.0120	3.9204	2.7940
6	0.0245	4.0461	0.63900
7	0.0120	3.8579	-0.97600
8	0.0245	3.9836	8.7700
9	0.0370	3.9217	0.55300
mean	0.0246	3.9836	1.9003

V. Initial Tradespace Exploration

In this section, the single objective problem will be addressed. The single objective is to minimize the pointing error. Here, the control loop is added, and all 45 mirror positions are available for each siderostat (instead of only the nine outermost in the previous section). The most interesting design points will be ones with the outermost and innermost siderostat positions. Table 3 shows the pointing error results at some interesting design configurations. Each column corresponds to a different run. K1, K2, and K3 are the proportional, integral, and derivative control gains, respectively, and Vs is the rms shaker voltage.

Table 3. Interesting Design Points

	Run 1	Run 2	Run 3	Run 4	Run 5	Run 6	Run 7
Vs (V)	1.0	1.0	1.0	1.0	1.0	1.0	0.5
K1	1	1	500	500	1	1	1
K2	1	1	500	1	500	1	1
K3	1	1	500	1	1	500	1
position	inner	outer	outer	outer	outer	outer	outer
PEe-4(m)	5.0908	6.5685	6.5647	6.5714	6.5686	6.5647	3.2843

By moving the mirrors in, the pointing error is reduced by 22 percent (runs 1 and 2). This is a significant reduction, but expected, since the longer the light travels, the more off-center the beam will be on the CCD camera due to structural vibrations. In run 3, the values of the control gains were kept equal, and in subsequent runs, one of these gains was kept at the high level, and lowered the others. It seems that K3 was able to lower the pointing error the most. Recall that K3 is the gain for the derivative control. It is not clear what combination of gains will produce the best answer - this will be explored in depth later using a gradient search. Notice also that the value of the input voltage (Vs) was cut by half in the last run. This significantly lowered the pointing error which is expected since there is less disturbance input into the system. The control gain constraint ($K \leqslant 100$) is violated in some of the cases, but was done used illustrate the effects of the gain values. Another way to implement control gain constraints would be to constrain the phase or gain margins of the controlled system (not performed here). It is important to check the optical pathlength constraint ($OPL > 3$m). In the innermost mirror positions it is 3.1m, so that constraint is not violated for any designs. This constraint value could be raised such that constraint would be active for some designs.

The most important open issue for this project is the computation time. It takes 45 seconds to evaluate one design. This is due to the eigenvalue computation in the FEM in the structural block. Another issue is the fact that some of the design variables are continuous (control gains), and some are discrete (mirror

positions). For this reason, a heuristic technique would be the best way in which to explore the design space.

VI. Gradient Based Optimization and Sensitivity Analysis

A finite element model breaks large structural parts into small discrete ones. For this reason, there are only discrete points on which the mirrors can be mounted. Therefore instead of making the mirror positions continuous, they will be held constant at the outermost position in this optimization. In this way, a gradient search can be performed only on the control gains. In addition, the computation time problem is averted, since the eigenvalues only need to be calculated once and saved (the structure remains the same). For the subsequent heuristic search, the mirror positions will be changed at each iteration and computation time will be an issue.

Sequential quadratic programming (SQP)[4] will be used as the gradient search algorithm. The main issue with regards to this gradient search is the calculation of the gradient vector and Hessian matrix. The simulation is reduced to one large LTI system in MATLAB®. The MATLAB® function *fmincon* will be used, which makes use of the SQP algorithm, and uses quasi-Newton methods to approximate the Hessian. In addition, the user is able to specify constraints on the design variables. Since the nominal value of the pointing error is so small, it was scaled up by a factor of 10^5. The constraints that were defined bounded the gain values by 100 as the upper limit. The starting values for K1, K2, and K3 were widely varied. After optimization (see Table 4), the values for K1 and K2 stay about the same, however, the value for K3 is always optimized to the upper constraint value of 100.

Table 4. Gradient Based Search Results

	Run 1	Run 2	Run 3
Starting K's	50	10	0.01
K1	49.9941	9.0138	0.001
K2	50	10	0.0039
K3	100	100	100
iterations	7	11	2
PE $\times 10^4$ (m)	6.5647	6.5647	6.5647

K3 is the gain for the derivative control, and it seems to be the most important one. The optimal objective value seems to be invariant with K1 and K2 out to the 7th decimal point (in meters). As long as K3 is 100, PE will always be 6.5647×10^{-4} m in this physical design configuration. The algorithm did iterate, so there was an improvement in the design from the initial design vector. For example, the initial design vector where all the control gains were 10, resulted in a pointing error of 6.56505×10^{-4} m. It was then optimized over 11 iterations to produce the pointing error (shown) of 6.5647×10^{-4} m. The best solution seems to be the one with K3 at the maximum possible value, and K2 slightly larger than K1.

Considering the center solution as the optimal solution ($\underline{x}^*$), the normalized sensitivity with respect to $\underline{x}$ (here the design vector of control gains) can be calculated using the gradient provided by the function *fmincon*.

$$\frac{\partial J(\underline{x}*)}{\partial K1}_{NORM} = 6.0 \times 10^{-9}$$
$$\frac{\partial J(\underline{x}*)}{\partial K2}_{NORM} = 0.0$$
$$\frac{\partial J(\underline{x}*)}{\partial K3}_{NORM} = -5.853 \times 10^{-6}$$

Using finite differences, the normalized sensitivities with respect to input voltage (Vs), and bus mass (Mp) can be obtained. These are two fixed parameters of the system.

$$\frac{\partial J(\underline{x}*)}{\partial Vs}_{NORM} = 9.9010e-5$$
$$\frac{\partial J(\underline{x}*)}{\partial m_p}_{NORM} = 12.3893$$

In terms of design variables (control gains), K3 seems to have the largest effect on the objective. Since its normalized sensitivity is negative, increasing the value of K3 will produce a reduction in pointing error. This makes sense, since the optimum value of K3 (in the gradient search) was always at its upper boundary (100). However, its sensitivity at the optimum point is very small in the absolute sense. The sensitivity to mirror positions might be very much larger. Notice that the sensitivities with respect to K1 and K2 are zero or very close to zero. This matches Table 4 which shows very different values for K1 and K2, but the same values for both K3 and pointing error. The sensitivities with respect to the two parameters Vs and Mp are both positive. This is intuitive, because increasing the bus mass or increasing the input voltage would amplify the magnitude of the vibrations in the system, and therefore increase the pointing error. It seems that the system is much more sensitive to bus mass than it is to input voltage. This is something that is not immediately intuitive, and illustrates why sensitivity as a post-process is important in understanding a complex system.

The one active constraint is the one on the upper bound of the third control gain (K3). This can be observed by looking at the converged design, or by finding the non-zero Lagrangian multiplier. Fortunately, the function *fmincon* outputs these multipliers. For Run 2 in Table 4, the converged solution has K3 = 100, and the multipliers for the constraints on the control gains are

$$\lambda_{K1}= 0.0, \lambda_{K2}= 0.0, \lambda_{K3}= 3.843 \times 10^{-6}$$

When the constraint on K3 is moved to an upper bound of 200, and the optimization routine is rerun, the pointing error is 65.6468e-5 m with a design vector of

$$\text{K1} = 7.9255,\ \text{K2} = 10.0,\ \text{K3} = 200.0$$

This confirms that K3 will most likely always push against its upper bound. It also shows that only a very small improvement in pointing error is possible even with a large increase in K3. In addition, the sensitivity with respect to K2 that was calculated above was zero, and is confirmed here, since the value of K2 started at and remained at 10.

Clearly, this shows that the value of K3 is the most important design variable in this optimization, and that the objective is minimized when K3 is maximized. In this particular structural configuration, this value of pointing error is most probably the global optimum that can be reached. However in the heuristic search when the placement of the mirrors can be varied, this value is considerably lowered.

VII. Heuristic System Design Optimization

In this optimization, the structural variation in the design vector (movement of siderostat mirrors) will be added, since it is easier to incorporate the integer nature of the structural design variables in a heuristic search. This will significantly widen the design space. Whether or not this differs significantly from the gradient search depends on whether the structures or the control have the greatest effect on the system performance. It is possible and important to be able to add more objectives to this problem. For example, pointing error could be minimized, optical pathlength could be maximized, and the optical pathlength difference could be minimized. This type of multi-objective function would be very interesting to see, since these are intuitively conflicting objectives, and because it represents very well the type of scientific optimization that would be done on an interferometer. A multi-objective design optimization can be seen in the next section. A genetic algorithm will be employed as the heuristic search technique in this section.

A genetic algorithm[5] will be used, since it can encode integer and floating point values easily. In addition, computation time of a single simulation evaluation is about 45 seconds, therefore the number of function evaluations should be small. This can be done using a judicious choice of population size and mutation rate. Also, a genetic algorithm introduces randomness so the algorithm can jump into separated optimum points in my design space not attainable via the gradient method.

The main difference between this optimization and the gradient optimization is that here the structural variation (two additional design variables) is introduced. Therefore the optimizer should be able to get very different optimal solutions. Since each simulation evaluation takes so long, a small population size (5) and a modest mutation rate (0.01) were chosen, and the GA toolbox for MATLAB® was used (see Table 5). Starting at an initial population of K3 = 50, M1 = 10, M2 = 10, the GA produced a value of 3.897×10^{-5} m. This is a great improvement over the earlier cases where the structural design was fixed in the outermost

configuration. This converged in five generations. It is interesting that the mirrors were not at the extremes of their placements, nor was the control gain pushed to the maximum for this converged solution. Intuitively the PE should be worse for outer mirror positions with the same disturbance source; for the same angular displacement of the light path, the more off-center the light will be on the CCD plane. But this does not seem to be the case here. This could be due to the optimizer placing the optical elements close to a node in the modeshape (i.e. where there is near zero displacement).

A major trait of the gradient search was that the derivative control gain was pushed to the maximum. Since the population size was so small in the first attempt, it was be increased to 20, and similarly the mutation rate increased to 0.03. This took 36 minutes and three iterations to converge to a solution with a pointing error of 3.978×10^{-5} m. This is not as optimal as the previous solution. It is interesting to see here that the gain value for the K3 control gain is very small (1.3). This is probably due to the fact that the structure has a much bigger effect on PE than the control gain. A third run with population size of 10 and mutation rate of 0.02 was attempted. This optimization took only 12 minutes and returned an objective value of 4.167×10^{-5} m. Again, this is not as optimal as the first solution.

Table 5. Single Objective Genetic Algorithm Results

	Run 1	Run 2	Run3
pop. size	5	20	10
mutation rate	0.01	0.03	0.02
max no. gen	20	20	20
iterations	5	19	9
K3	66.54	1.3077	4.5274
M1	3	7	44
M2	32	35	11
PE $\times 10^5$ (m)	3.897	3.978	4.167

VIII. Multiobjective Design Optimization Results

The two objectives chosen for the multiobjective optimization are minimization of the pointing error and to maximization of the optical pathlength. The optical pathlength difference will be retained as a constraint. Intuitively, one would assume that these are opposing objectives. Pointing error measures the spread of the two beams of light on a collecting surface target. The longer the distance over which each light beam travels (optical pathlength), the larger the spread of the beam on the target. It will be crucial to decide on which multi-objective method to use, because no matter which one is chosen, it will probably favor one over the other. The weighted sum approach is used to combine the two objectives into one.

$$\mathrm{J} = \lambda * (-\mathrm{PE}) * 10^5 + (1-\lambda) * \mathrm{OPL} \tag{2}$$

The pointing error (PE) in this equation is negative because the genetic algorithm is set to maximize the value of J. The PE is scaled by 10^5 in order bring it to the same scale as the OPL. The relative weighting of the two objectives can be varied via a sweep of the variable λ. A genetic algorithm optimization is then run for each value of λ (using the same starting conditions as above). This simulation took approximately seven hours to run. The three design variables are derivative control gain, and two mirror placements. Figure 6 is a chart that maps shows the optimal solutions obtained at each value of λ, and it shows an interesting trend.

First of all, the objectives seem to be bounded within about +/- 1 m of their respective means. The objective here is to maximize OPL, while minimizing PE. Looking at the solution where $\lambda = 0.6$, there is a high value for OPL and a low value for PE. With $\lambda = 0.9$, we have a low value for OPL and a high value for PE. This would contradict my earlier conjecture that these two objectives are mutually opposing. One way to look at a pareto- front would be to plot the two objectives against each other, as in Figure 7.

Notice that only two of these points can be considered to be lying on the pareto-front (circled). This indicates that there might be a problem with the simulation or with the optimization algorithm. If however,

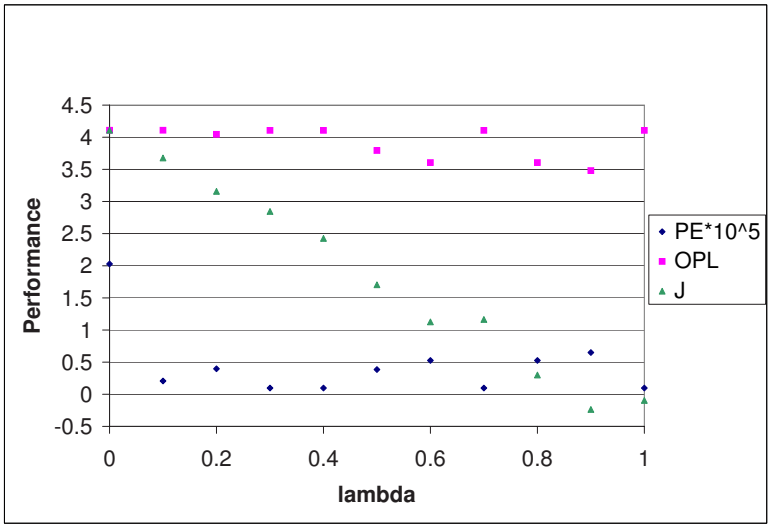

Figure 6. Performance vs. λ

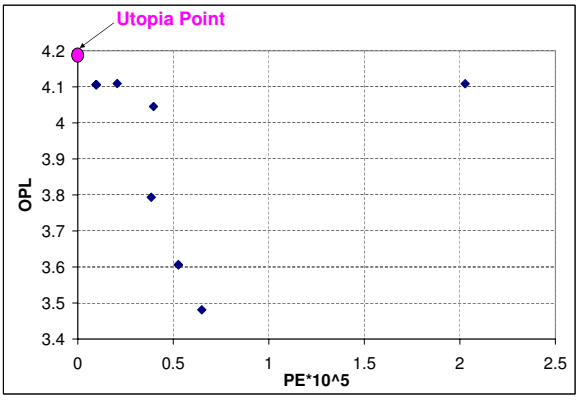

Figure 7. Pareto Front

these reflect the system accurately, these two points are extremely favorable with respect to both objectives.

One would expect the trend for the control gain to be monotonically increasing with increasing λ, since more and more emphasis is being put on PE as the dominant objective in the weighted sum scheme (recall that this control loop can only control PE and not OPL). However, it seems that the control gain varies widely, as can be seen in Figure 8. Also, the mirror positions as a function of λ were interesting. No matter what the value for λ, the mirrors were almost always at extreme inner or outer positions.

The one scale factor that was used was to multiply the pointing error by 10^5. This makes both the pointing error and the optical pathlength on the order of about one meter. Using finite differencing, and setting $\lambda = 0.4$, the GA can be run (with PE scaled by 10^6), the sensitivities with respect to the scaling are

$$\left|\frac{\partial OPL}{\partial Scale}\right| = -0.6089$$
$$\left|\frac{\partial PE}{\partial Scale}\right| = 268.1485.$$

It seems that the optimum result for the pointing error would have changed significantly if the scaling were changed. Of course this value for sensitivity can only be truly believed if it is known that the global optimum is obtained. Since a GA is being used, and not a full factorial search, we cannot be sure that these sensitivities are true.

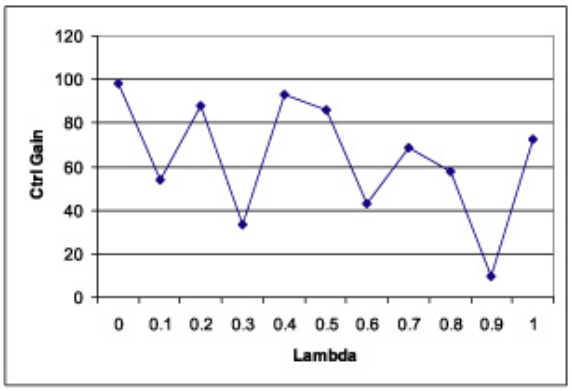

Figure 8. Control Gain vs λ

Using the results from Figure 6 and finite differencing the normalized sensitivities of the performance with respect to λ at the point $\lambda = 0.4$ are

$$\left|\frac{\partial OPL}{\partial \lambda}\right| = -0.1522$$
$$\left|\frac{\partial PE}{\partial \lambda}\right| = 5.9735$$

The relative sizes of these two values indicate that the pointing error performance is affected much more than the optical pathlength for the same increase in λ . Also, the signs of the sensitivities make sense, because as can be seen in Figure 6, at $\lambda = 0.4$, PE increases and OPL decreases.

IX. Conclusions

This simulation implementation shows that the two objectives of minimizing the pointing error and maximizing the optical pathlength are not necessarily opposing for all designs. Also, when applying these objectives the placement of the siderostat mirrors tends to be on the extreme edges of the breadboards. It has been shown that when considering both sets of design variables (mirror positions and control gain values), the mirror positions are the most influential on the objectives, and that the control gain values do not contribute very much. However, when fixing the structure and analyzing the role of each type of control gain, it has been shown that derivative control is by far the most influential on the pointing error objective. As the derivative control value increases, the pointing error decreases. The pointing error stays virtually the same with changing proportional and integral control gains.

In addition, the pointing error has shown to be much more sensitive to the bus mass than to the shaker voltage. This is a prime example of the non-intuitive insight that can be gained through simulation. Also, pointing error has been shown to be very sensitive to the multi-objective weightings.

When combining the discrete positions of the mirrors and the continuous values of the control gain, a gradient method is awkward, since results must be rounded. The use of a genetic algorithm allows the developer to use mixed integers easily. Using the genetic algorithm in this way shows that there is no definite pareto-front for these chosen objectives. This is due to the fact that the two objectives are not always opposing.

X. Work To Be Completed

Future work to be completed for the final paper includes applying simulated annealing to this problem. Simulated annealing will introduce randomness into the heuristic problem and might be more efficient. In addition, different variations on the genetic algorithm problem could be run in order have more confidence that the final result is a global optimum. Experimental validation and benchmarking are also important

and necessary steps for the validation of this work. Finally an overall comparison of gradient search, genetic algorithm, and simulated annealing methods as applied to this problem will be performed.

References

[1]Olivier de Weck and Karen Willcox. 16.888 Multidisciplinary System Design Optimization, MIT Course Notes. 2003.

[2]Olivier L. de Weck. *Mulitvariable Isoperformance Methodology for Precision Opto-Mechanical Systems*. Ph.d., Massachusetts Institute of Technology, August 2001.

[3]Olivier de Weck Deborah Howell. Experimental validation of multidisciplinary isoperformance methodology. In *Proceedings of the 9th AIAA/ISSMO Symposium on Multidisciplinary Analysis and Optimization, Atlanta, Georgia*, 2002.

[4]W. Murray Gill, P.E. and M.H. Wright. *Practical Optimization*. Academic Press, 1986.

[5]D.E. Goldberg. *Genetic Algorithms in Search, Optimization and Machine Learning*. Addison Wesley, 1989.

[6]Homero L. Gutierrez. *Performance Assessment and Enhancement of Precision Controlled Structures During Conceptual Design*. PhD thesis, Massachusetts Institute of Technology, Department of Aeronautics and Astronautics, 1999.

[7]Jet Propulsion Laboratory. *Integrated Modeling of Optical Systems User's Manual*, January 1998. JPL D-13040.

[8]NASA JPL. Space interferometry mission. Internet: http://sim.jpl.nasa.gov, accessed 5-4-2003 2003.

[9]Brett P. Masters. *Evolutionary Design of Controlled Structures*. Ph.d., Massachusetts Institute of Technology, 1997.

[10]M. Shao. Overview of SIM. *Bulletin of the American Astronomical Society*, 33, May 2001.

[11]Garret N. Vanderplaats. *Numerical Optimization Techniques for Engineering Design*. Vanderplaats Research and Development Inc, 3rd edition, 2001.

[12]A. Zalzala and P.J. Fleming. *Genetic Algorithms in Engineering Systems*. Control Engineering Series 55. The Institution of Electrical Engineers (IEE), 1997.